Characterization of top-down ETD in a travelling-wave ion guide

Title page:

Title: Characterization of top-down ETD in a travelling-wave ion guide

Authors: Frederik Lermyte[1,2], Tim Verschueren[1], Jeffery M. Brown[3], Jonathan P. Williams[3], Dirk Valkenborg[2,4,5], Frank Sobott[1,2]

[1]Biomolecular & Analytical Mass Spectrometry group, Department of Chemistry, University of Antwerp, Antwerpen, Belgium

[2]UA-VITO Center for Proteomics, University of Antwerp, Antwerpen, Belgium

[3]Waters Corporation, Stamford Avenue, Wilmslow, UK SK9 4AX

[4]Interuniversity Institute for Biostatistics and Statistical Bioinformatics, Hasselt University

[5]Applied Bio & Molecular Systems, Flemish Institute for Technological Research (VITO)

Correspondence to: Frank Sobott; e-mail: frank.sobott@uantwerpen.be

Present address: Groenenborgerlaan 171, 2020 Antwerp, Belgium

Abstract:

Top-down sequencing methods are becoming increasingly relevant for protein characterization, in particular electron capture (ECD) and electron transfer dissociation (ETD) which allow for extensive backbone cleavage with minimal side reactions. The ability to obtain sequence-specific fragments while maintaining aspects of the higher-order structure, as well as the position of deuterium labels in H/D exchange, has attracted interest from scientists in the field of structural proteomics. Recently, ETD has also been combined with ion mobility on commercially available quadrupole/time-of-flight instruments, and this implementation paves the way to novel structural studies and investigation of the ETD process itself. In the current work, we investigate the use of ETD for fragmentation of standard peptides and proteins and provide a detailed description of the effect of the parameters controlling the time and efficiency of the reaction. We also highlight how the combination with ion mobility separation after electron transfer provides extended analytical benefits, such as assignment of fragments to a specific charge-reduced state of the precursor.

Keywords: Top-down mass spectrometry, intact protein mass spectrometry, top-down sequencing, electron transfer dissociation, ion mobility

Highlights

*ETD on a Synapt instrument allows efficient top-down fragmentation of peptides and proteins

*Charge reduction reactions lead to low fragment charge states, simplifying assignment

*Extent of ion-ion reactions is mainly controlled by T-Wave amplitude and velocity

*Ion mobility coupling allows fragment assignment to a specific precursor

1. Introduction

Recently, the field of structural proteomics benefits increasingly from the development of novel approaches in mass spectrometry (MS), which aim to combine detailed information on the sequence of proteins with aspects of their higher-order structure and interactions. The advantages of MS, as a method for structural biology, further include the low sample consumption and speed of analysis, allowing for example the study of dynamic phenomena and proteins which do not crystallize easily[1]. Native MS approaches, utilizing ion mobility as an adjunct parameter for the determination of size and shape of proteins and complexes, rely on the preservation of the global fold in vacuo, with recent impressive results across the field from amyloid aggregation to large, integral membrane protein assemblies. An orthogonal, complementary strategy utilizes in vitro modification of native proteins or complexes in solution, followed by non-native analysis in vacuo typically using bottom-up MS approaches – for instance in the case of hydrogen-deuterium exchange, crosslinking and covalent labeling[2-5]. Recently, the use of hybrid methods which combine native and non-native analyses with computational methods was demonstrated for structural modeling of noncovalent protein complexes[6]. We anticipate that top-down strategies, with both native and denatured protein, will play an increasingly important role in such integrative approaches, with their unique capability to correlate detailed aspects of protein sequences with higher-order structure. Growing interest in the identification, quantification and structural characterization of known and unknown protein variants, collectively known as proteoforms, has also renewed interest in top-down MS sequencing[7-10]. Electron based dissociation methods, i.e. electron capture dissociation (ECD)[11, 12] and electron transfer dissociation (ETD)[13], have proven to be valuable tools in top-down proteomics, particularly when studying heavily post-translationally modified proteins[14-18]. This in itself makes these methods valuable tools for structural biology, as the precise form in which a protein occurs (e.g. sequence variants or its PTM state) can have a significant effect on its folding state and interaction with other biomolecules. ECD and ETD dissociation typically lead to the formation of *c* and *z* ions (with a minor, alternative dissociation channel leading to *a* and *y* fragments), in contrast to the *b* and *y* ions formed by collision-induced dissociation (CID). While proteins are typically denatured in solution, with the aim to maximize information regarding the primary structure, native proteins have also been investigated by ECD. In these studies, it has been found that this dissociation technique has the ability to cleave the backbone of a protein while preserving not only labile post-translational modifications, but also elements of the higher-order structure. This ability to obtain sequence information without completely obliterating the native fold, holds great promise for the study of conformationally dynamic proteins, e.g. in amyloid aggregation or intrinsically disordered proteins.

The method has consequently been used to study the gas-phase structure, unfolding and refolding of monomeric proteins[19-25], as well as noncovalent complexes[26-30]. In ECD of large, noncovalent complexes, a correlation between the observed fragmentation pattern and structural parameters, in particular the crystallographic B factor, has been proposed[31]. Similarly, ETD has been used to study protein structure in the gas phase[32], and we recently reported that the ETD fragmentation pattern of the native alcohol dehydrogenase tetramer reflects the solvent-accessibility of residues[33]. Other novel fragmentation techniques have also proven valuable for structural biology applications, as ultraviolet photodissociation (UVPD) has been shown to be capable of similar selective fragmentation behavior to ECD/ETD[34-36], and surface-induced dissociation (SID) can also provide information

about subunit connectivity in a noncovalent protein complex[37]. While high resolution ion trap instruments are now also suitable for the transmission and MS/MS analysis of native proteins and protein complexes [38, 39], there are extended analytical benefits provided by combining these capabilities with ion mobility (IM), on quadrupole/time-of-flight (QTOF) mass spectrometers. These instrument platforms have become powerful and versatile tools for structural proteomics, especially when coupled with H/D exchange and different fragmentation techniques. The commercially available Synapt instruments (Waters, Wilmslow, UK) enable ETD on a Q-IM-TOF platform in a way which has already been described for peptides, proteins, and noncovalent complexes[33, 40, 41]. In contrast to ETD-enabled ion traps, the reaction occurs here in a travelling-wave (T-Wave) ion guide, so that the exact duration of the ETD reaction is not set directly in these instruments. Instead, the reaction can be conveniently regulated by adjusting the height of the travelling wave voltage. Here we study key control parameters of the top-down ETD reaction on a Synapt platform, in particular how the T-Wave parameters affect the extent and duration of cation-anion interaction. In particular, we explore a mode whereby the ETD reaction duration is directly controlled, without requiring either hardware or software modifications. In the current work, we use standard peptides and proteins of different sizes to demonstrate the capacity of an ETD-capable Synapt G2 instrument to induce extensive top-down fragmentation, and show that significant non-dissociative charge reduction accompanies the observed fragmentation. As the aim in this case was to investigate the degree of backbone cleavage, we used primarily denatured charge states of the proteins in these experiments. Furthermore, we systematically investigate the effect of selected instrument parameters and provide an explanation for the observed fragmentation behavior based on reagent concentrations and reaction times. This improved understanding of experimental top-down ETD control parameters will pave the way to obtaining more detailed information on sequence and higher-order structure of large proteins including native, non-covalent complexes of biological interest.

2. Materials and methods

Substance P (Sigma S6883, 1.4 kDa), ubiquitin (*Bos taurus*, Sigma U6253, 8.6 kDa), and myoglobin (*Equus caballus*, Sigma M0630, 16.9 kDa) were dissolved at a concentration of 4 µM in water/acetonitrile v/v 50/50 and 1% formic acid added. Approximately 5 µL of this solution was transferred to an gold-coated glass capillary prepared in-house and infused into the mass spectrometer using the nanoflow version of the Z-spray ion source, with a capillary voltage of 1.2 – 1.6 kV, minimal (< 0.2 bar) nanoflow gas pressure, a backing pressure of 2.4 mbar and a source pressure of 1.6e-3 mbar.

The Synapt instrument[42] used in this study, as well as the implementation of ETD[43], have been described in detail elsewhere. A diagram in Figure 1 summarizes the experimental setup. Briefly, ETD reagent (1,4-dicyanobenzene) vapor is carried by a nitrogen flow at room temperature to the glow discharge needle located between the sampling cone and extraction cone, where radical anions are generated. The polarity of the ion optics up to and including the entrance of the trap cell is continuously switched, and the quadrupole is set to transmit only the ETD reagent signal in negative ion mode. After filling the T-wave trap cell with ETD reagent for 0.1 s, it is trapped there and allowed to interact for 1.0 s with the nano-ESI generated analyte cations, before the cycle starts again. Cation precursors and reaction products are axially propelled through the ETD "cloud" in the trap cell by means of a travelling wave, the amplitude ('height') and velocity of which determine the extent and time of ion-ion interaction. The intervals of 0.1 s and 1.0 s, respectively for anions and cations, should not be confused with the ion-ion reaction time, which is typically a few tens of milliseconds depending on the T-wave parameters (see below).

The glow discharge was tuned to provide a signal of approximately 2e6 reagent counts per second (make-up gas flow 35 mL/min, discharge current 20 µA). Instrument settings were as follows: sampling cone 60 V, extraction cone 2 V, trap pressure 6.2e-2 mbar, trap collision energy 4 V, trap DC bias 8 V, transfer pressure 1.2e-2 mbar. To provide supplemental activation, the transfer collision energy was set to 20 V for top-down ETD (except for substance P, where this was not necessary and set to 2 V). The instrument was operated in Sensitivity mode and fitted with a 32 K quadrupole. For top-down ETD followed by ion mobility separation, the IM cell was pressurised with 2.5 mbar of N_2 (He cell gas flow 140 mL/min, IM gas flow 60 mL/min), with IM wave height 40 V and IM wave velocity 1000 m/s. Transfer pressure and collision energy in IM mode were increased to 3.7e-2 mbar and 60 V, respectively. Significant horizontal 'streaking' in the 2D (arrival time versus *m/z*) plot was initially observed in these experiments, possibly due to trapping inefficiencies, and it was found to be critical to lower the trap wave height below 0.4 V to avoid this. Uncalibrated drift times are reported in this study, and mobilograms are shown displaying the full 200-bin drift time range. For IM of cesium iodide, the instrument was operated in CID mode and the IM cell was filled with 3.1 mbar of N_2 (He cell gas flow 180 mL/min, IM gas flow 90 mL/min). The IM wave height in this case was kept constant at 10 V. For relative peak intensity measurements, the spectrum was smoothed (2x three-channel Savitsky-Golay method[44]) and centered using MassLynx (version 4.1). The intensities of the peaks of interest (see Supplementary S-1) were subsequently exported and expressed as a fraction of the summed intensities over the entire measured *m/z* range. Finally, the relative intensities for each ion over the entire parameter range were rescaled to a similar maximum intensity, in order to display the evolution of the peak intensity for multiple ion types more clearly. For reliable (relative) quantitation, it was important that the signals have a high signal-to-noise (S/N) ratio. Top-down

spectra were therefore acquired on this older, less sensitive Synapt instrument for around one minute (i.e. longer than the timescale of a typical LC peak) in order to increase this ratio, which is expected to be proportional to the square root of the number of scans combined. However, many fragments can already be identified after only a few seconds. For ETD of peptides, (near-)complete fragmentation is observed with a high S/N ratio already after a few seconds.

3. Results and discussion

3.1 Characteristics of Synapt ETD

In the first part of this study, we assessed the performance of ETD, as implemented on the Synapt G2 instrument, to induce extensive backbone fragmentation. We used substance P, a 1.3 kDa peptide, as well as two denatured proteins (ubiquitin; 8.6 kDa and apo-myoglobin; 16.9 kDa) as test compounds, and were able to achieve highly efficient fragmentation, particularly in the terminal regions, similar to what is typically reported in top-down ECD/ETD in ion traps[19, 45-47]. The 3+ precursor of substance P shows cleavage of eight out of ten N-Cα bonds, with the remaining two on the N-terminal side of proline and thus immune to ETD fragmentation (as the resulting 'fragments' remain bound via the pyrrolidine side chain). For ubiquitin (9+ precursor), 64 out of 75 bonds were cleaved, with three of the remaining nine cleavage followed by proline. In the case of 18+ apo-myoglobin with its four proline residues, 72 out of 152 backbone bonds were cleaved. Representative top-down ETD spectra as well as observed sequence coverage for ubiquitin and apo-myoglobin are shown in Figure 2, and a Synapt ETD spectrum of substance P can be found in the Supplementary Information (S-5). Important control parameters for (top-down) ETD and their typical values (leading to maximum sequence coverage) are summarized in Table 1. The effect of varying these parameters is investigated systematically in section 3.2. It is important to note that the ETD fragments appear at relatively low charge states compared to typical top-down ECD results[19, 47, 48]. Significant non-dissociative charge reduction is also visible in these spectra, indicating that the proton transfer reaction (PTR) and non-dissociative electron transfer (ETnoD) accompany fragmentation. Evidence for the occurrence of both of these reactions is provided by the observed isotope distributions, which simultaneously broaden and shift to higher *m/z* compared to the ions formed by electrospray ionization (See Supplementary S-2). The reason for this is that PTR of an $[M+nH]^{n+}$ precursor generates even-electron $[M+(n-1)H]^{(n-1)+}$ ions just like ESI itself, while ETnoD produces $[M+nH]^{(n-1)+\bullet}$ radicals which retain the proton mass, but not the charge. From the observed isotope distributions in S-2, it becomes apparent that PTR and ETnoD occur concomitantly. However, the precise ratio between these competing reactions depends in part on the choice of reagent, and preference for either electron or proton transfer is believed to be associated with the Franck-Condon factor and electron affinity[49, 50]. Other important factors determining the extent to which electron transfer leads to non-dissociative charge reduction are the size and structure of the precursor, as at least some of the observed ETnoD product ions could actually consist of *c* and *z* ions which remain noncovalently bound. The stability of this fragment complex is dependent on factors such as the remaining higher-order structure and Coulombic repulsion between the fragments[19, 20, 33, 51-57]. A more in-depth analysis of different ETD processes leading to charge reduction, and how they depend on precursor charge state, instrument parameters, etc. is currently underway in our laboratory.

As mentioned, in order to maximize the sequence coverage achieved in top-down ETD, it is important to provide sufficient supplemental activation (ion acceleration into the argon pressurized region) in the transfer cell so that all fragments are released. Top-down ETD spectra of denatured ubiquitin using varying levels of transfer cell collision energy are shown in Supplementary S-3. The effect of this additional post-ETD ion acceleration is twofold: First, transmission of high *m/z* species is improved (particularly for large cross-section, low charge species with low ion mobility), as can be seen from the increased intensity of charge-reduced intact precursor and the presence of heavy ETD fragments.

Second, *c*- and *z*-type fragments are released from ETnoD products in the transfer cell by supplemental activation[33, 51-57]. Evidence for the release of ETD fragments which remained noncovalently bound to each other is provided by ion mobility experiments, as shown in Figure 3. In this experiment, intact 6+ ubiquitin was subjected to top-down ETD and the resulting products were separated in the IM cell prior to supplemental activation. The reason for choosing the 6+ precursor in this case was twofold: First of all, because there are more noncovalent interactions present in this relatively compact ion, the intensity of the charge-reduced (ETnoD) product – at least some of which is actually a noncovalent complex of a *c*/*z* fragment pair – is quite high. Second, as the degree of conformational heterogeneity in the 6+/5+/4+/3+ range is rather low for ubiquitin – all form compact structures, particularly if gentle ionization conditions are used[58] – baseline ion mobility separation of the 3+ species from the others is conveniently achieved. It can be seen that most of the fragments have arrival times similar to the (charge-reduced) precursors, indicating that they were released either before IM separation, or from the highly charged precursor in the transfer cell. Certain fragments however (highlighted in the green box in the 2D plot in Figure 3) clearly share the arrival time of the 3+ ubiquitin, proving that they were only released after IM separation due to supplemental activation. In order to ensure efficient release of noncovalently bound ETD fragments from the 3+ charge-reduced ubiquitin, the voltage for supplemental activation was increased to the point where the higher charge states – as a result of picking up more energy after acceleration across the same voltage difference – started to exhibit efficient CID fragmentation. Consequently, the low-arrival time spectrum (orange box) shows predominantly *b* and *y* ions, while the high-arrival time mass spectrum (green box) yields a 'pure' ETD spectrum, with a high signal-to-noise ratio. Most of the fragments in this spectrum are also singly charged, possibly accounting for at least some of the low-charged fragments we typically observe in Synapt ETD.

3.2 Systematic investigation of important control parameters

As the ETD reaction occurs in a travelling-wave device, the main control parameters which determine the extent and the duration ('reaction time') of cation-anion interaction are the amplitude ('height') and velocity of the trap T-Wave[33, 43]. The reaction is typically controlled by adjusting the wave height, as a lower wave height allows for more mixing of the ions, resulting initially (as the voltage decreases) in non-dissociative charge reduction of the precursor. Further reduction of the wave height leads to more efficient fragmentation, as shown in the ubiquitin spectra in Figure 4, and the substance P and apo-myoglobin spectra in Supplementary S-4. Use of an extremely low voltage may result in significant neutralization of fragments, resulting in a reduction of the total ion current (data not shown). Interestingly, we observed that adjusting the wave velocity to a value either significantly lower or higher than the default (300 m/s) while keeping the wave height high (1.50 V) also leads to initially charge reduction and then fragmentation, as observed when lowering the wave height. This can be explained as follows: in the normal wave velocity regime, a high wave keeps the analyte and reagent ions bunched together in regions of low and high electric potential, respectively, decreasing the local ('effective') reagent ion concentration. In contrast, a low wave height allows ions to spread out by 'rolling over' the wave, similar to the well-known phenomenon in travelling-wave ion mobility spectrometry[42, 59, 60], leading to more effective mixing of both ion types and simultaneously increasing the residence time of the analyte ions in the trap cell. This effect can typically be observed at wave heights of ca. 1.3 V or lower in top-down experiments, while efficient charge reduction and

fragmentation tend to occur mostly below 0.5 V. In the high-wave height regime, the use of a very low wave velocity leads to minimization of the effect of roll-over, and as a result, although the effective reagent concentration might stay low, the reaction time can be easily set to very high values. As the reaction time now becomes approximately equal to the length of the trap cell (18 cm) divided by the wave velocity, this corresponds to a reaction time between 18 and 1.8 ms as we increase the wave velocity from 10 to 100 m/s. Conversely, at a very high wave velocity, the occurrence of roll-over increases significantly, increasing both the mixing of both ion types and the reaction time.

This view is substantiated by a more systematic study of the effect of these two parameters on charge reduction and fragmentation of 9+ ubiquitin (isolated in the quadrupole). In Figure 5 (a-d), the relative intensities (calculated as described in the Materials and methods section) of the 9+ ubiquitin precursor, charge-reduced protein signals and some ETD-fragments are shown as a function of wave height and velocity (with the latter on a logarithmic scale, to cover the range of 10 – 6000 m/s). The intensity of a set of 25 ions, which were selected based on their favorable signal-to-noise ratio across multiple spectra (See Supplementary S-1), was monitored in this experiment, and some examples which represent N- and C-terminal fragments of different sizes and charge states are displayed in Figure 5. Figure 5a shows the evolution of different nominal charge states (products of charge reduction). Successive maxima for decreasing charge are observed as the wave height is lowered, following the trend predicted by the model described above. Likewise, in Figure 5b, as we move further away from the default wave velocity of 300 m/s to either lower or higher values, successive maxima for charge-reduced ubiquitin charge states are observed. In Figure 5c, the effect of the wave height on ETD fragment intensities is shown. As expected, fragments generally become more intense at lower wave height, although it is worth mentioning that the multiply charged fragments achieve a maximum at higher wave heights, and therefore less ion-ion interaction, than the smaller, singly charged fragments. This phenomenon will be discussed in more detail below. Similar behavior is observed in the plot of fragment intensity versus log. wave velocity shown in Figure 5d. As expected, the total fragment intensity increases at lower wave heights and also at very low and high wave velocities, as shown in Figures 5e and 5f. Total precursor (9+ and charge-reduction products combined) intensity follows the opposite behavior, as expected. It bears repeating at this point that the data shown in Figure 5f were acquired using a wave height of 1.50 V, which is why no fragmentation is observed at 'intermediate' wave velocities, including the default value of 300 m/s. Conversely, at a reduced wave height, use of the default wave velocity does result in efficient fragmentation, as displayed in Figure 5e. Confirmation of our hypothesis concerning the effect of 'extreme' wave velocities on the residence time of ions in the T-Wave trap cell via a direct measurement is unfortunately not possible. We can qualitatively show this effect by recording IM-MS spectra of CsI while varying the IM travelling wave velocity. The resulting plot of Cs^+ ion arrival time vs. log. wave velocity is shown in Supplementary S-5, displaying the expected U-shape, i.e. ions traversing the T-Wave cell fastest at medium wave velocities (provided that the amplitude of the wave is sufficiently high).

In Figure 6, the relative intensities of intact protein and ETD fragments of apo-myoglobin (18+ precursor selected in the quadrupole) are shown as a function of wave height (at a constant wave velocity of 300 m/s) and log. wave velocity (at a constant wave height of 1.50 V), similar to the ubiquitin data shown in Figure 5(a-d). The trends observed here are the same. The z_{55} fragment occurs at four different charge states (2+ to 5+), and the order in which these appear depends on the

travelling wave parameters in the same way as the charge-reduced precursors. The appearance of successively lower charge states with increased 'reaction time' indicates that the fragments observed under typical ETD conditions are the product of multiple reaction steps, the majority of which lead to non-dissociative charge reduction. Precursor charge state and fragment intensities for substance P (3+ precursor selected) are shown in Supplementary S-6, along with a representative spectrum. Trends observed for substance P product ion yields match those for the proteins studied here. The maximum intensity of the c_9^{2+} fragment is observed under conditions which allow less ion-ion interaction than those which favor c_9^{+}, showing that this behavior is also not unique to intact proteins.

Another parameter which controls the extent of ion-ion interaction is radial confinement of the ions, which is provided by the amplitude of the RF voltage applied to the ring electrodes in the trap cell. This voltage needs to be greater than ca. 50 V in order to achieve transmission at all, and an increase leads to more extensive ion-ion interaction (Supplementary S-7), similar to a decrease in wave height. All of the same trends concerning charge reduction, fragmentation, and fragment charge states described for the trap T-Wave height are observed here as well. It seems likely that this is due to the ions being confined to a smaller volume with increasing trap RF amplitude, increasing their 'effective' local concentration.

The pressure of the background gas also plays an important role in mediating ion-ion interactions: According to a commonly cited general mechanism for gas-phase ion-ion chemistry[61], the reaction between analyte cations and reagent anions progresses within a stable orbiting complex, the formation of which occurs with a rate constant that is inversely proportional to the square of the relative velocity of both interaction partners. Hence, the probability of formation for this complex is greatly increased when the ions are slowed down by collisions with an inert gas. Reducing the relative velocity of the ions after the formation of the orbiting complex is also beneficial, as this leads to a decreased orbit and higher probability of proton or electron transfer[62]. The choice of helium as the background gas has several advantages, besides its chemical inertness: First of all, the low mass results in minimal conversion of kinetic into internal energy of the ions and hence minimizes unintentional collision-induced dissociation[63]. Collisional scattering of the ions, which could potentially destroy the complex in which the reaction occurs, is also decreased with a low-mass background gas[61]. Finally, the reduced center-of-mass collision energy leads to improved trapping efficiency of the ETD reagent, which can otherwise transfer its electron to a background gas molecule. Formation of the cation-anion complex can also lead to a third type of charge reduction besides electron or proton transfer, namely attachment of the reagent anion[61, 64]. In the Synapt instrument, the resulting adducts can be detected, particularly when a precursor with a low charge state is used (Supplementary S-8). As expected based on the mechanism described above, plots of 9+ ubiquitin charge reduction and fragmentation versus trap gas flow give evidence for more extensive cation-anion interaction at higher pressure, similar to the effect of a reduction in wave height (see Figure 7). The decrease in precursor intensity at very low pressure seen in this figure is explained by increased CID fragmentation, as well as reduced collisional cooling, resulting in expansion of the ion beam and less efficient transmission of ions through the ion guide.

Finally, it is expected that the ratio between the number of anions and cations present in the trap cell also plays a role. It is advisable to tune for approximately 1e4 analyte counts/s, and 1e6 reagent ion counts/s. We varied the ratio between analyte cations (9+ ubiquitin) and reagent anions entering the

trap by adjusting the quadrupole transmission window for the precursor (making transmission of the precursor less efficient) and the glow discharge current (varying the ETD reagent intensity). This resulted in the ubiquitin cation count varying between 5e3 and 2e4 counts/s, and the reagent anion count between 3e5 and 6e6. The results of these experiments can be seen in Supplementary S-9. In general, it seems that as long as there is a significant (approximately 100-fold or greater) excess of anions, the ETD reaction can progress efficiently, while the absolute number of charge carriers present plays only a secondary role. However, as expected, a reduction of this ratio leads to far less extensive cation-anion interaction.

4. Conclusions

The advent of electron-based dissociation techniques such as ECD has opened up new possibilities for top-down and structural proteomics, not least due to their ability to sequence the peptide backbone while maintaining aspects of the higher-order structure. The development of ETD has enabled this type of experiment on instruments other than FT-ICR, thereby making this approach accessible to a wider range of scientists. In recent years, the availability of ETD on QTOF instruments has the advantage of relatively high resolution, while coupling with ion mobility paves the way to studies which link 3D structural information with the observed fragmentation patterns. In agreement with earlier work, the ability to apply post-ETD or post-IMS supplemental activation was found to be crucial for the release of fragments from the more structured parts of a protein, and facilitates in-depth studies of the multistep fragmentation mechanism.

Although the cation-anion interaction time is not directly programmable on the QTOF, the reaction can be easily controlled by adjusting one parameter only, the wave amplitude. As this amplitude is lowered, the extent of the ion-ion interaction increases. We have also studied other parameters, such as the wave velocity and ion confinement, and qualitatively explained the relative abundance of fragment ions obtained. Ion-ion reactions lead to both electron and proton based charge reduction at the same time, along with dissociation from the former, in a multi-step process. Combined with the capacity to detect high *m/z* ions, this leads to the observation of relatively low fragment charge states and simplified data interpretation.

In top-down studies, particularly of larger proteins or complexes, a detailed understanding of ETD reaction tuning becomes increasingly important in order to maintain good fragment ion yields. Understanding of how these parameters affect the observed charge reduction and fragmentation behavior is crucial to tune for the behavior necessary in a specific experiment and to maximize the information obtained from ETD experiments. As this understanding increases, we expect that the use of top-down ETD in combination with ion mobility will become more widespread in structural proteomics studies.

Acknowledgements

We thank the Research Foundation – Flanders (FWO) for funding a PhD fellowship (F.L.). The Synapt G2 mass spectrometer is funded by a grant from the Hercules Foundation – Flanders. Financial support from the Flemish Institute for Technological Research (VITO) is gratefully acknowledged.

Figure 1: Diagram of the layout of the Synapt G2 instrument used in this study, depicting the positions of the electrospray ionization (ESI) source, glow discharge (GD), quad(rupole) mass filter, trap, ion mobility and transfer T-Wave cells, and the time-of-flight (TOF) analyzer. The inset shows the structure of the reagent (1,4-dicyanobenzene) and its quadrupole-selected mass spectrum. Under the conditions used, the first isotope peak of the reagent is also transmitted and, as expected, has an intensity of around 10% of the signal at *m/z* 128.

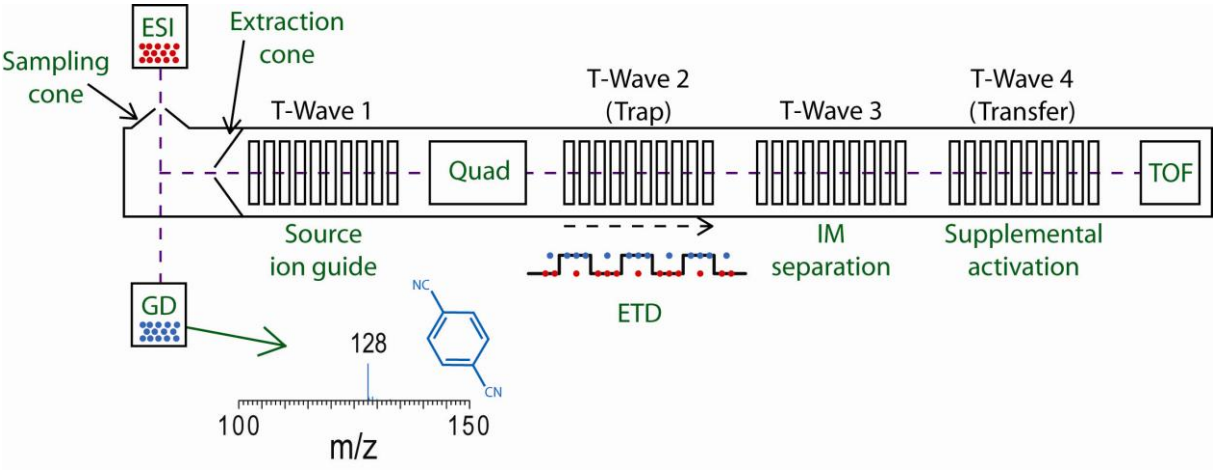

Figure 2: Top-down ETD spectrum of (a) 9+ bovine ubiquitin; (b) 18+ myoglobin. The insets show the sequence and fragmentation pattern. Singly, doubly, triply, and quadruply charged fragments (the most intense one is indicated in case a fragment appears at multiple charge states) are indicated in red, green, purple, and black, respectively.

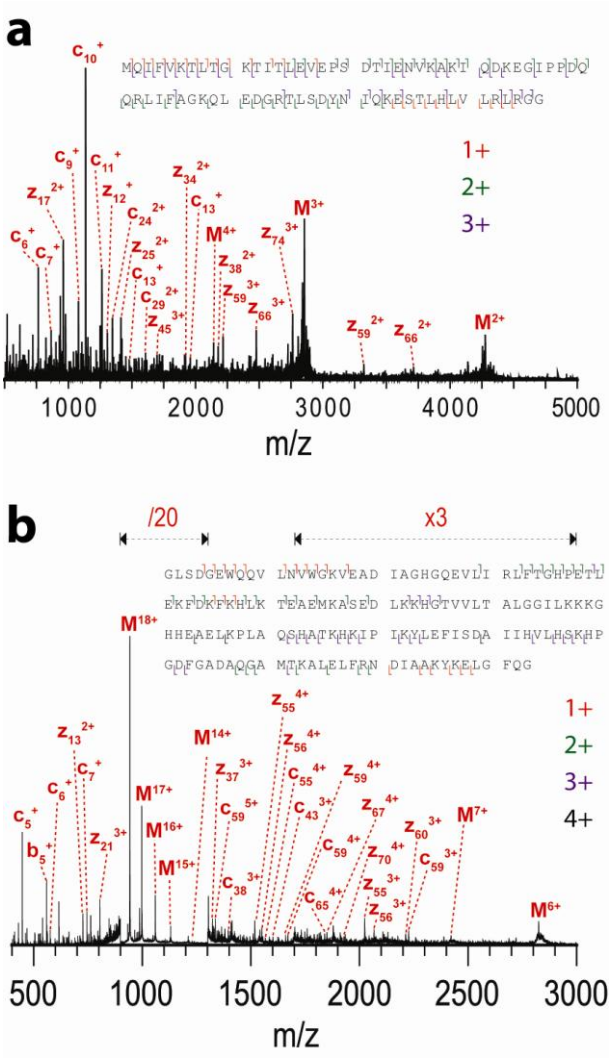

Figure 3: Charge reduction of 6+ ubiquitin in top-down ETD in ion mobility mode, represented as a 2D-plot. The mobilogram is displayed on the right of the 2D plot, and it can be seen that the arrival time distributions of 6+, 5+, and 4+ ubiquitin overlap, while the 3+ peak is clearly separated from the higher charge states as well as fragments released before IM separation. Abundant fragment ions are released in the transfer cell (visible to the left of the corresponding precursor charge state). Below the 2D plot, the top mass spectrum shows the (ETD) fragments released from 3+ ubiquitin (green box in the 2D plot) and the bottom spectrum shows the (mainly CID) fragments released from the higher charge states (orange box in 2D).

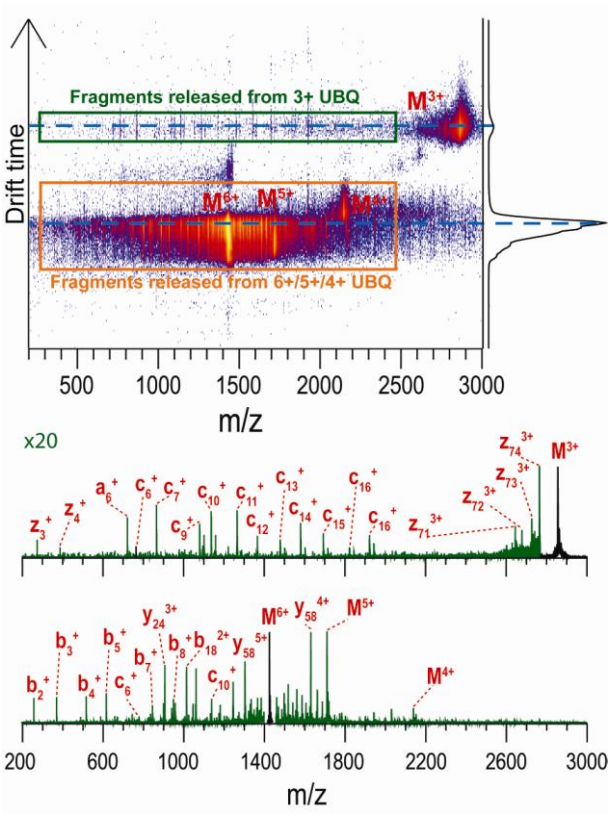

Figure 4: Top-down ETD of 9+ ubiquitin with (a) wave height 1.50 V, wave velocity 300 m/s; (b) wave height 1.30 V, wave velocity 300 m/s; (c) wave height 1.20 V, wave velocity 300 m/s; (d) wave height 0.30 V, wave velocity 300 m/s; (e) wave height 1.50 V, wave velocity 10 m/s; (f) wave height 1.50 V, wave velocity 3000 m/s

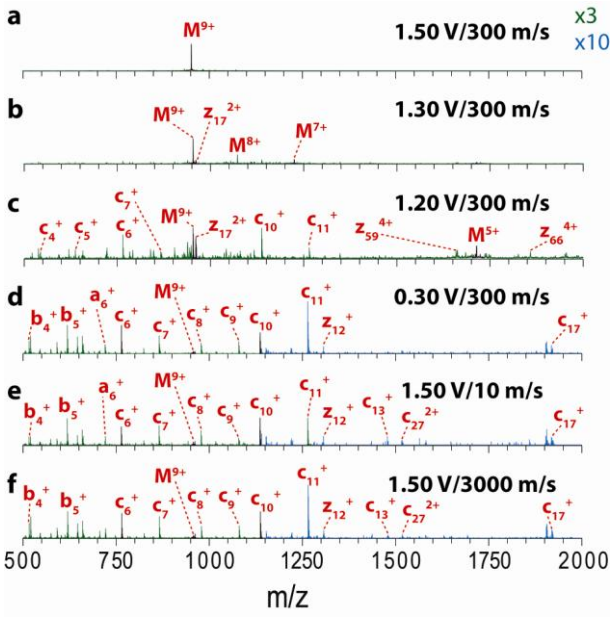

Figure 5: Plots of (a) ion yield of selected ubiquitin charge states (9+ precursor and charge-reduction products) versus wave height (wave velocity = 300 m/s); (b) selected ubiquitin charge states versus log. wave velocity (wave height = 1.50 V); (c) selected ubiquitin fragments versus wave height (velocity = 300 m/s); (d) selected ubiquitin fragments versus log. wave velocity (height = 1.50 V); (e) relative intensities of intact (including charge reduced species) ubiquitin and ETD fragments versus wave height (velocity = 300 m/s); (f) relative intensities of intact precursor (including charge reduced species) ubiquitin and ETD fragments versus log. wave velocity (height = 1.50 V). The 9+ precursor was isolated in the quadrupole in all of these experiments. The default wave velocity of 300 m/s corresponds to log (WV) = 2.5.

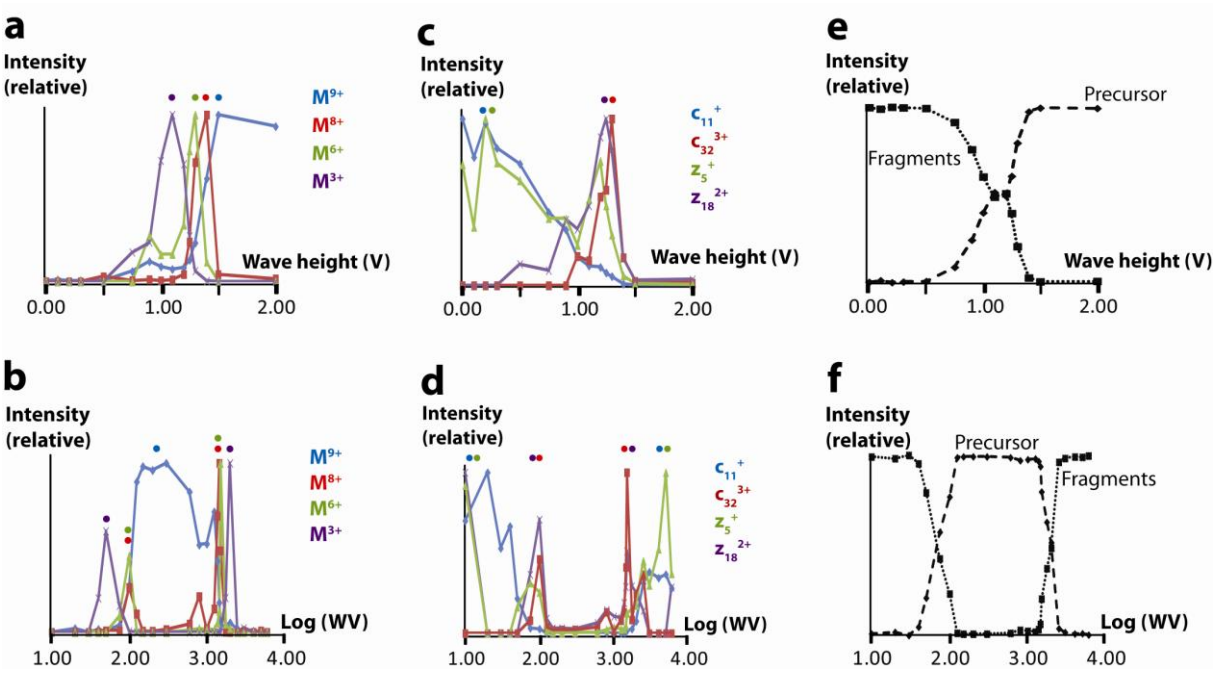

Figure 6: selected charge states of apo-myoglobin (18+ precursor and products of non-dissociative charge reduction) versus (a) wave height (wave velocity = 300 m/s) and (b) log. wave velocity (wave height = 1.50 V); selected apo-myoglobin ETD fragments versus (c) wave height (wave velocity = 300 m/s) and (d) log. wave velocity (wave height = 1.50 V)

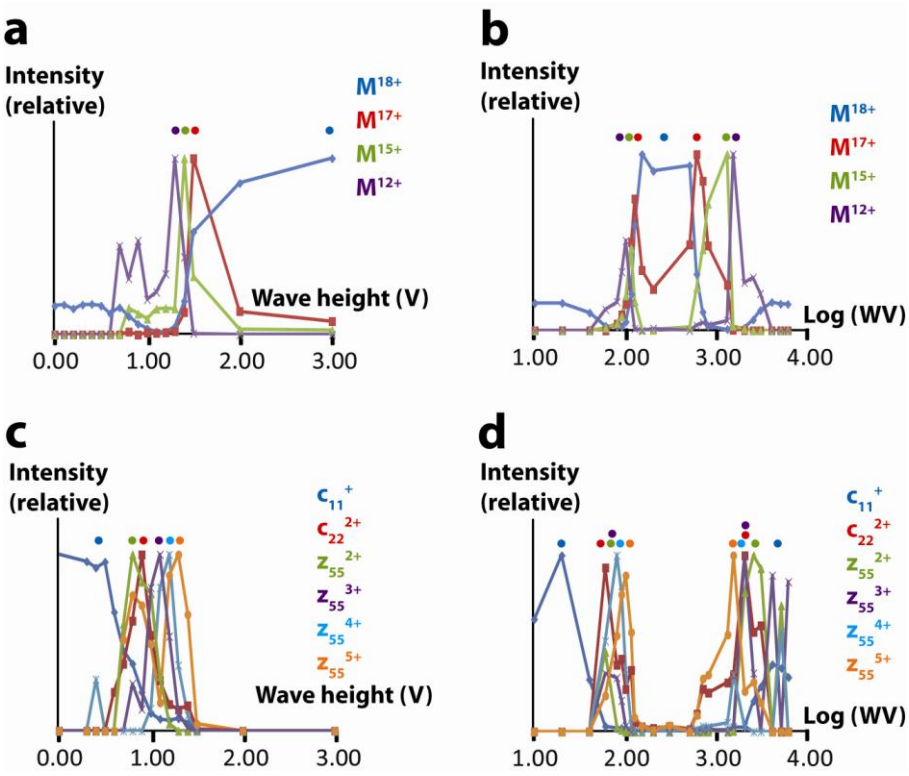

Figure 7: Effect of trap He gas flow on charge reduction and fragmentation of 9+ ubiquitin. The table shows the measured pressure at the different gas flows investigated (normal operating regime shown in bold). The trap T-wave height and velocity were kept constant at 0.50 V and 300 m/s, respectively.

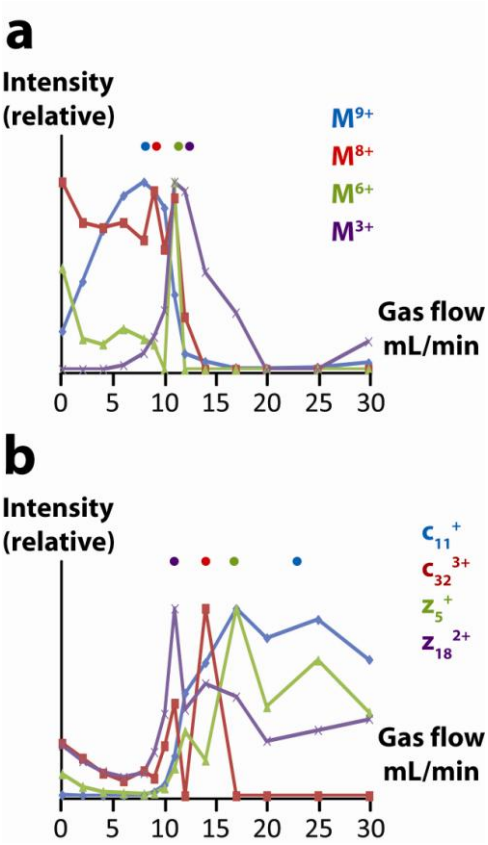

He flow (mL/min)	Pressure (mbar)
0	8.86e-5
2	6.28e-3
4	1.26e-2
6	1.90e-2
8	2.53e-2
9	2.81e-2
10	3.14e-2
11	3.42e-2
12	3.73e-2
14	4.33e-2
17	5.21e-2
20	**6.12e-2**
25	7.65e-2
30	9.09e-2

Table 1: Important parameters for ETD optimization

Parameter	Effect	Typical value
Trap wave height	Control of ion/ion reaction time	< 0.35 V
Trap wave velocity	Control of ion/ion reaction time	300 m/s
Trap pressure	Collisional cooling of ions	(5e-2) – (7e-2) mbar
Trap RF amplitude	Increase of effective ion concentration	450 – 530 V
Transfer collision energy	Provides supplemental activation	5 – 20 V
Reagent:analyte ratio	Reagent excess needed for multistep process	100 – 200

References

[1] Hyung, S.J., Ruotolo, B.T.: Integrating mass spectrometry of intact protein complexes into structural proteomics, Proteomics **12**, 1547-1564(2012)

[2] Konijnenberg, A., Butterer, A., Sobott, F.: Native ion mobility-mass spectrometry and related methods in structural biology, Biochimica et biophysica acta **1834**, 1239-1256(2013)

[3] Fitzgerald, M.C., West, G.M.: Painting proteins with covalent labels: what's in the picture?, J Am Soc Mass Spectrom **20**, 1193-1206(2009)

[4] Serpa, J.J., Parker, C.E., Petrotchenko, E.V., Han, J., Pan, J., Borchers, C.H.: Mass spectrometry-based structural proteomics, Eur J Mass Spectrom **18**, 251-267(2012)

[5] Iacob, R.E., Engen, J.R.: Hydrogen exchange mass spectrometry: are we out of the quicksand?, J Am Soc Mass Spectrom **23**, 1003-1010(2012)

[6] Politis, A., Stengel, F., Hall, Z., Hernandez, H., Leitner, A., Walzthoeni, T., Robinson, C.V., Aebersold, R.: A mass spectrometry-based hybrid method for structural modeling of protein complexes, Nat Methods **11**, 403-406(2014)

[7] Kelleher, N.L., Lin, H.Y., Valaskovic, G.A., Aaserud, D.J., Fridriksson, E.K., McLafferty, F.: Top down versus bottom up protein characterization by tandem high-resolution mass spectrometry, J Am Chem Soc **121**, 806-812(1999)

[8] Tran, J.C., Zamdborg, L., Ahlf, D.R., Lee, J.E., Catherman, A.D., Durbin, K.R., Tipton, J.D., Vellaichamy, A., Kellie, J.F., Li, M., Wu, C., Sweet, S.M., Early, B.P., Siuti, N., LeDuc, R.D., Compton, P.D., Thomas, P.M., Kelleher, N.L.: Mapping intact protein isoforms in discovery mode using top-down proteomics, Nature **480**, 254-258(2011)

[9] Smith, L.M., Kelleher, N.L., Proteomics, C.T.D.: Proteoform: a single term describing protein complexity, Nature Methods **10**, 186-187(2013)

[10] Dang, X.B., Scotcher, J., Wu, S., Chu, R.K., Tolic, N., Ntai, I., Thomas, P.M., Fellers, R.T., Early, B.P., Zheng, Y.P., Durbin, K.R., LeDuc, R.D., Wolff, J.J., Thompson, C.J., Pan, J.X., Han, J., Shaw, J.B., Salisbury, J.P., Easterling, M., Borchers, C.H., Brodbelt, J.S., Agar, J.N., Pasa-Tolic, L., Kelleher, N.L., Young, N.L.: The first pilot project of the consortium for top-down proteomics: A status report, Proteomics **14**, 1130-1140(2014)

[11] Zubarev, R.A., Kelleher, N.L., McLafferty, F.: Electron capture dissociation of multiply charged protein cations. A nonergodic process, J. Am. Chem. Soc. **120**, 3265-3266(1998)

[12] Zubarev, R.A., Horn, D.M., Fridriksson, E.K., Kelleher, N.L., Kruger, N.A., Lewis, M.A., Carpenter, B.K., McLafferty, F.W.: Electron capture dissociation for structural characterization of multiply charged protein cations, Anal Chem **72**, 563-573(2000)

[13] Syka, J.E., Coon, J.J., Schroeder, M.J., Shabanowitz, J., Hunt, D.F.: Peptide and protein sequence analysis by electron transfer dissociation mass spectrometry, Proc Natl Acad Sci U S A **101**, 9528-9533(2004)

[14] Fornelli, L., Damoc, E., Thomas, P.M., Kelleher, N.L., Aizikov, K., Denisov, E., Makarov, A., Tsybin, Y.O.: Analysis of intact monoclonal antibody IgG1 by electron transfer dissociation Orbitrap FTMS, Mol Cell Proteomics **11**, 1758-1767(2012)

[15] Tian, Z., Tolic, N., Zhao, R., Moore, R.J., Hengel, S.M., Robinson, E.W., Stenoien, D.L., Wu, S., Smith, R.D., Pasa-Tolic, L.: Enhanced top-down characterization of histone post-translational modifications, Genome biol. **13**, R86(2012)

[16] Garcia, B.A., Shabanowitz, J., Hunt, D.F.: Characterization of histones and their post-translational modifications by mass spectrometry, Curr Opin Chem Biol **11**, 66-73(2007)

[17] Wiesner, J., Premsler, T., Sickmann, A.: Application of electron transfer dissociation (ETD) for the analysis of posttranslational modifications, Proteomics **8**, 4466-4483(2008)

[18] Sobott, F., Watt, S.J., Smith, J., Edelmann, M.J., Kramer, H.B., Kessler, B.M.: Comparison of CID versus ETD based MS/MS fragmentation for the analysis of protein ubiquitination, J Am Soc Mass Spectrom **20**, 1652-1659(2009)

[19] Breuker, K., Oh, H.B., Horn, D.M., Cerda, B.A., McLafferty, F.W.: Detailed unfolding and folding of gaseous ubiquitin ions characterized by electron capture dissociation, J Am Chem Soc **124**, 6407-6420(2002)
[20] Horn, D.M., Breuker, K., Frank, A.J., McLafferty, F.W.: Kinetic intermediates in the folding of gaseous protein ions characterized by electron capture dissociation mass spectrometry, J Am Chem Soc **123**, 9792-9799(2001)
[21] Breuker, K., McLafferty, F.W.: The thermal unfolding of native cytochrome c in the transition from solution to gas phase probed by native electron capture dissociation, Angew Chem Int Ed Engl **44**, 4911-4914(2005)
[22] Lin, C., Cournoyer, J.J., O'Connor, P.B.: Probing the gas-phase folding kinetics of peptide ions by IR activated DR-ECD, J Am Soc Mass Spectrom **19**, 780-789(2008)
[23] Skinner, O.S., McLafferty, F.W., Breuker, K.: How ubiquitin unfolds after transfer into the gas phase, J Am Soc Mass Spectrom **23**, 1011-1014(2012)
[24] Schennach, M., Breuker, K.: Proteins with Highly Similar Native Folds Can Show Vastly Dissimilar Folding Behavior When Desolvated, Angew Chem Int Edit **53**, 164-168(2014)
[25] Zhang, H., Cui, W.D., Gross, M.L.: Native electrospray ionization and electron-capture dissociation for comparison of protein structure in solution and the gas phase, Int J Mass Spectrom **354**, 288-291(2013)
[26] Xie, Y., Zhang, J., Yin, S., Loo, J.A.: Top-down ESI-ECD-FT-ICR mass spectrometry localizes noncovalent protein-ligand binding sites, J Am Chem Soc **128**, 14432-14433(2006)
[27] Jackson, S.N., Dutta, S., Woods, A.S.: The Use of ECD/ETD to Identify the Site of Electrostatic Interaction in Noncovalent Complexes, J Am Soc Mass Spectr **20**, 176-179(2009)
[28] Clarke, D.J., Murray, E., Hupp, T., Mackay, C.L., Langridge-Smith, P.R.: Mapping a noncovalent protein-peptide interface by top-down FTICR mass spectrometry using electron capture dissociation, J Am Soc Mass Spectrom **22**, 1432-1440(2011)
[29] Kalapothakis, J.M.D., Berezovskaya, Y., Zampronio, C.G., Faull, P.A., Barran, P.E., Cooper, H.J.: Unusual ECD fragmentation attributed to gas-phase helix formation in a conformationally dynamic peptide, Chem Commun **50**, 198-200(2014)
[30] Zhang, H., Cui, W., Wen, J., Blankenship, R.E., Gross, M.L.: Native electrospray and electron-capture dissociation in FTICR mass spectrometry provide top-down sequencing of a protein component in an intact protein assembly, J Am Soc Mass Spectrom **21**, 1966-1968(2010)
[31] Zhang, H., Cui, W.D., Wen, J.Z., Blankenship, R.E., Gross, M.L.: Native Electrospray and Electron-Capture Dissociation FTICR Mass Spectrometry for Top-Down Studies of Protein Assemblies, Anal Chem **83**, 5598-5606(2011)
[32] Zhang, Z., Browne, S.J., Vachet, R.W.: Exploring salt bridge structures of gas-phase protein ions using multiple stages of electron transfer and collision induced dissociation, J Am Soc Mass Spectrom **25**, 604-613(2014)
[33] Lermyte, F., Konijnenberg, A., Williams, J.P., Brown, J.M., Valkenborg, D., Sobott, F.: ETD Allows for Native Surface Mapping of a 150 kDa Noncovalent Complex on a Commercial Q-TWIMS-TOF Instrument, J Am Soc Mass Spectrom **25**, 343-350(2014)
[34] O'Brien, J.P., Li, W., Zhang, Y., Brodbelt, J.S.: Characterization of native protein complexes using ultraviolet photodissociation mass spectrometry, J Am Chem Soc **136**, 12920-12928(2014)
[35] Warnke, S., Baldauf, C., Bowers, M.T., Pagel, K., von Helden, G.: Photodissociation of conformer-selected ubiquitin ions reveals site-specific cis/trans isomerization of proline peptide bonds, J Am Chem Soc **136**, 10308-10314(2014)
[36] Warnke, S., von Helden, G., Pagel, K.: Analyzing the higher order structure of proteins with conformer-selective ultraviolet photodissociation, Proteomics, (2015)
[37] Blackwell, A.E., Dodds, E.D., Bandarian, V., Wysocki, V.H.: Revealing the Quaternary Structure of a Heterogeneous Noncovalent Protein Complex through Surface-Induced Dissociation, Anal Chem **83**, 2862-2865(2011)
[38] Rose, R.J., Damoc, E., Denisov, E., Makarov, A., Heck, A.J.: High-sensitivity Orbitrap mass analysis of intact macromolecular assemblies, Nat Methods **9**, 1084-1086(2012)

[39] Rosati, S., Rose, R.J., Thompson, N.J., van Duijn, E., Damoc, E., Denisov, E., Makarov, A., Heck, A.J.: Exploring an orbitrap analyzer for the characterization of intact antibodies by native mass spectrometry, Angew Chem Int Ed Engl **51**, 12992-12996(2012)
[40] Rand, K.D., Pringle, S.D., Morris, M., Engen, J.R., Brown, J.M.: ETD in a Traveling Wave Ion Guide at Tuned Z-Spray Ion Source Conditions Allows for Site-Specific Hydrogen/Deuterium Exchange Measurements, J Am Soc Mass Spectr **22**, 1784-1793(2011)
[41] Mistarz, U.H., Brown, J.M., Haselmann, K.F., Rand, K.D.: Simple setup for gas-phase H/D exchange mass spectrometry coupled to electron transfer dissociation and ion mobility for analysis of polypeptide structure on a liquid chromatographic time scale, Anal Chem **86**, 11868-11876(2014)
[42] Pringle, S.D., Giles, K., Wildgoose, J.L., Williams, J.P., Slade, S.E., Thalassinos, K., Bateman, R.H., Bowers, M.T., Scrivens, J.H.: An investigation of the mobility separation of some peptide and protein ions using a new hybrid quadrupole/travelling wave IMS/oa-ToF instrument, Int J Mass Spectrom **261**, 1-12(2007)
[43] Williams, J.P., Brown, J.M., Campuzano, I., Sadler, P.J.: Identifying drug metallation sites on peptides using electron transfer dissociation (ETD), collision induced dissociation (CID) and ion mobility-mass spectrometry (IM-MS), Chem Commun **46**, 5458-5460(2010)
[44] Savitzky, A., Golay, M.J.E.: Smoothing and Differentiation of Data by Simplified Least Squares Procedures, Anal Chem **36**, 1627-1639(1964)
[45] Kaplan, D.A., Hartmer, R., Speir, J.P., Stoermer, C., Gumerov, D., Easterling, M.L., Brekenfeld, A., Kim, T., Laukien, F., Park, M.A.: Electron transfer dissociation in the hexapole collision cell of a hybrid quadrupole-hexapole Fourier transform ion cyclotron resonance mass spectrometer, Rapid Commun Mass Spectrom **22**, 271-278(2008)
[46] McAlister, G.C., Phanstiel, D., Good, D.M., Berggren, W.T., Coon, J.J.: Implementation of electron-transfer dissociation on a hybrid linear ion trap-orbitrap mass spectrometer, Anal Chem **79**, 3525-3534(2007)
[47] Pan, J.X., Han, J., Borchers, C.H., Konermann, L.: Hydrogen/Deuterium Exchange Mass Spectrometry with Top-Down Electron Capture Dissociation for Characterizing Structural Transitions of a 17 kDa Protein, J Am Chem Soc **131**, 12801-12808(2009)
[48] Pan, J.X., Han, J., Borchers, C.H., Konermann, L.: Characterizing Short-Lived Protein Folding Intermediates by Top-Down Hydrogen Exchange Mass Spectrometry, Anal Chem **82**, 8591-8597(2010)
[49] Gunawardena, H.P., He, M., Chrisman, P.A., Pitteri, S.J., Hogan, J.M., Hodges, B.D., McLuckey, S.A.: Electron transfer versus proton transfer in gas-phase ion/ion reactions of polyprotonated peptides, J Am Chem Soc **127**, 12627-12639(2005)
[50] Williams, J.P., Pringle, S., Richardson, K., Gethings, L., Vissers, J.P., De Cecco, M., Houel, S., Chakraborty, A.B., Yu, Y.Q., Chen, W., Brown, J.M.: Characterisation of glycoproteins using a quadrupole time-of-flight mass spectrometer configured for electron transfer dissociation, Rapid Commun Mass Spectrom **27**, 2383-2390(2013)
[51] Pitteri, S.J., Chrisman, P.A., Hogan, J.M., McLuckey, S.A.: Electron transfer ion/ion reactions in a three-dimensional quadrupole ion trap: reactions of doubly and triply protonated peptides with SO2*, Anal Chem **77**, 1831-1839(2005)
[52] Swaney, D.L., McAlister, G.C., Wirtala, M., Schwartz, J.C., Syka, J.E., Coon, J.J.: Supplemental activation method for high-efficiency electron-transfer dissociation of doubly protonated peptide precursors, Anal Chem **79**, 477-485(2007)
[53] Xia, Y., Han, H., McLuckey, S.A.: Activation of intact electron-transfer products of polypeptides and proteins in cation transmission mode ion/ion reactions, Anal Chem **80**, 1111-1117(2008)
[54] Tsybin, Y.O., He, H., Emmett, M.R., Hendrickson, C.L., Marshall, A.G.: Ion activation in electron capture dissociation to distinguish between N-terminal and C-terminal product ions, Anal Chem **79**, 7596-7602(2007)
[55] Ganisl, B., Breuker, K.: Does Electron Capture Dissociation Cleave Protein Disulfide Bonds?, Chemstryopen **1**, 260-268(2012)

[56] Oh, H., Breuker, K., Sze, S.K., Ge, Y., Carpenter, B.K., McLafferty, F.W.: Secondary and tertiary structures of gaseous protein ions characterized by electron capture dissociation mass spectrometry and photofragment spectroscopy, Proc Natl Acad Sci U S A **99**, 15863-15868(2002)
[57] Lermyte, F., Williams, J.P., Brown, J.M., Martin, E.M., Sobott, F.: Extensive Charge Reduction and Dissociation of Intact Protein Complexes Following Electron Transfer on a Quadrupole-Ion Mobility-Time-of-Flight MS, J Am Soc Mass Spectrom, (2015)
[58] Valentine, S.J., Counterman, A.E., Clemmer, D.E.: Conformer-dependent proton-transfer reactions of ubiquitin ions, J Am Soc Mass Spectr **8**, 954-961(1997)
[59] Giles, K., Pringle, S.D., Worthington, K.R., Little, D., Wildgoose, J.L., Bateman, R.H.: Applications of a travelling wave-based radio-frequencyonly stacked ring ion guide, Rapid Commun Mass Spectrom **18**, 2401-2414(2004)
[60] Shvartsburg, A.A., Smith, R.D.: Fundamentals of Traveling Wave Ion Mobility Spectrometry, Anal Chem **80**, 9689-9699(2008)
[61] McLuckey, S.A., Stephenson, J.L., Jr.: Ion/ion chemistry of high-mass multiply charged ions, Mass Spectrom Rev **17**, 369-407(1998)
[62] Wells, J.M., Chrisman, P.A., McLuckey, S.A.: Formation and characterization of protein-protein complexes in vacuo, J Am Chem Soc **125**, 7238-7249(2003)
[63] Shukla, A.K., Futrell, J.H.: Tandem mass spectrometry: dissociation of ions by collisional activation, J Mass Spectrom **35**, 1069-1090(2000)
[64] Pitteri, S.J., McLuckey, S.A.: Recent developments in the ion/ion chemistry of high-mass multiply charged ions, Mass Spectrom Rev **24**, 931-958(2005)

Supplementary Information

S-1 List of ions for which the intensity was monitored

Substance P

Ion	*m/z* (monoisotopic)
M^{3+}	449.912
M^{2+}	674.364
M^{+}	1347.720
c_6^{+}	752.453
c_7^{+}	899.522
c_8^{+}	1046.590
c_9^{+}	1103.611
c_{10}^{+}	1216.706
z_9^{+}	1077.540
z_{11}^{+}	1330.693
c_9^{2+}	552.799

Ubiquitin

Ion	*m/z* (monoisotopic)
M^{9+}	952.076
M^{8+}	1070.96
M^{7+}	1223.81
M^{6+}	1427.611
M^{5+}	1712.931
M^{4+}	2140.912
M^{3+}	2854.213
M^{2+}	4280.816
c_6^{+}	764.449
c_7^{+}	865.497
c_{10}^{+}	1136.650
c_{11}^{+}	1264.745
c_{17}^{+}	1921.120
c_{24}^{2+}	1346.728
c_{27}^{2+}	1517.331
c_{32}^{3+}	1196.991
c_{38}^{3+}	1404.107
z_3^{+}	272.136
z_5^{+}	541.321
z_{17}^{2+}	959.056
z_{18}^{2+}	1040.587
z_{22}^{2+}	1248.683
z_{25}^{2+}	1412.757
z_{59}^{3+}	2214.176
z_{60}^{3+}	2247.199

Apo-myoglobin

Ion	*m/z* (monoisotopic)
M^{18+}	942.173
M^{17+}	997.535
M^{16+}	1059.818
M^{15+}	1130.405
M^{14+}	1211.077
M^{13+}	1304.159
M^{12+}	1412.755
M^{11+}	1541.096
M^{10+}	1695.104
c_{11}^{+}	1230.612
c_{12}^{+}	1344.655
c_{22}^{2+}	1207.112
c_{23}^{2+}	1235.622
c_{24}^{2+}	1304.152
c_{30}^{2+}	1623.831
c_{31}^{2+}	1701.882
z_{24}^{2+}	1349.208
z_{31}^{2+}	1672.343
z_{37}^{2+}	1982.987
z_{55}^{2+}	3034.083
z_{56}^{2+}	3098.131
z_{55}^{3+}	2023.058
z_{56}^{3+}	2065.756
z_{60}^{3+}	2211.503
z_{55}^{4+}	1517.545
z_{56}^{4+}	1549.569
z_{55}^{5+}	1214.238
z_{56}^{5+}	1239.857

S-2 Comparison of the observed isotope distribution of the nominal ubiquitin 4+ charge state formed by charge reduction and ESI

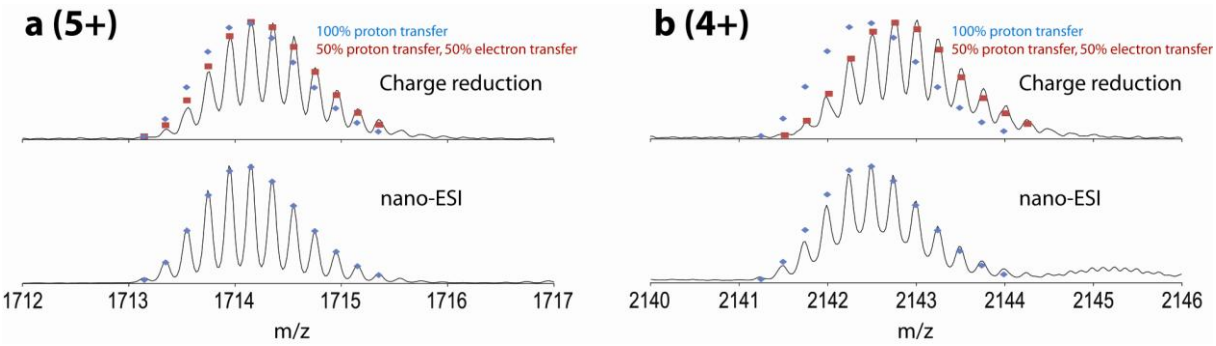

Isotope distributions observed after (top) charge reduction of 6+ ubiquitin and (bottom) native ESI, for the (a) 5+ and (b) 4+ charge state. In blue, the theoretical distribution of the $[M+nH]^{n+}$ product, formed by ESI or pure proton transfer is shown. In red, the expected isotope distribution is shown if 50% of the charge reduction occurs via proton transfer, and 50% via nondissociative electron transfer. Specifically, for the 5+ ion (one charge reduction step), this is 50% $[M+5H]^{5+}$ and 50% $[M+6H]^{5+\cdot}$, and for the 4+ ion, 25% $[M+4H]^{4+}$, 50% $[M+5H]^{4+\cdot}$, and 25% $[M+6H]^{4+\cdot\cdot}$.

S-3: Effect of supplemental activation in top-down ETD of 9+ ubiquitin

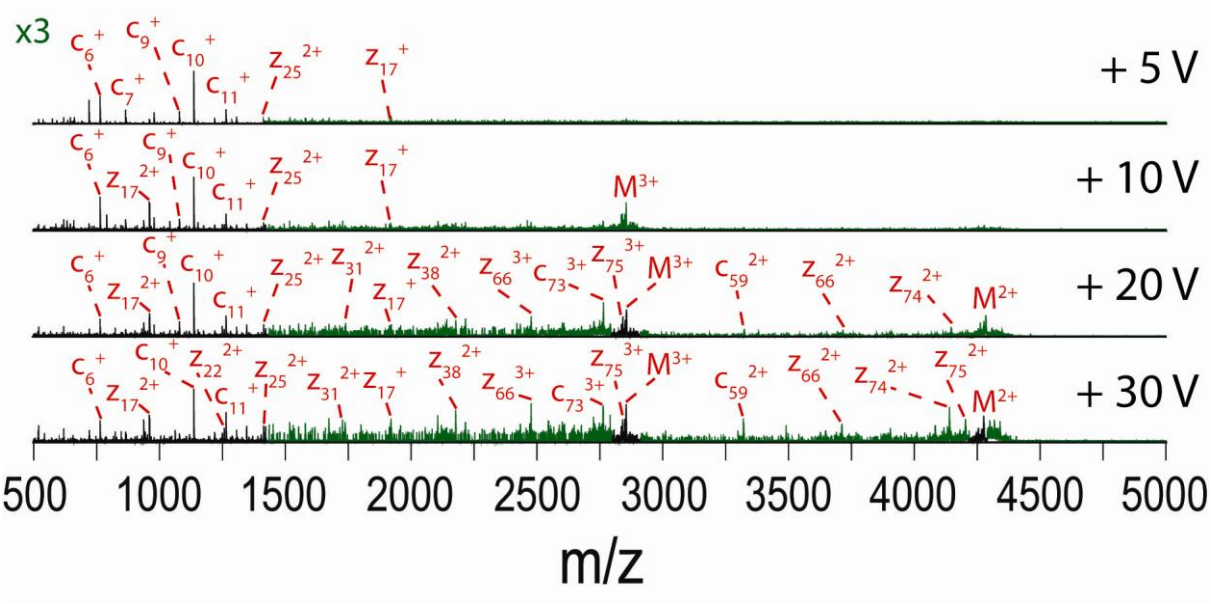

The spectra displayed here were acquired with a different degree of supplemental activation in the transfer cell (voltage offset shown on the right), but otherwise standard top-down ETD conditions were used as described in the Materials and methods section. Increased detection of large fragments and charge-reduced intact protein is observed with increasing supplemental activation.

S-4: Substance P and myoglobin ETD spectra under different T-Wave conditions

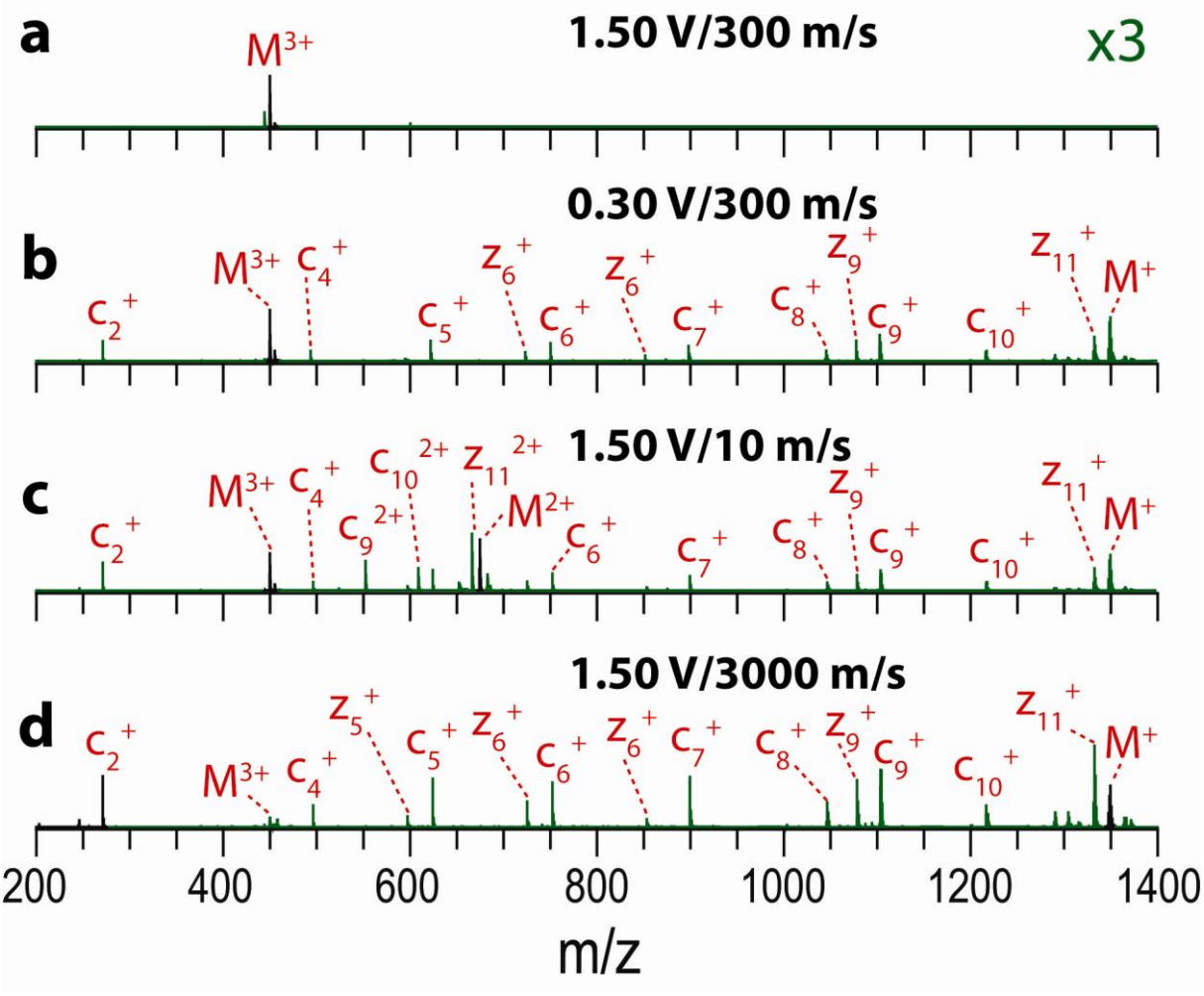

Substance P (3+) ETD spectra at (a) wave height 1.50 V, wave velocity 300 m/s; (b) wave height 0.30 V, wave velocity 300 m/s; (c) wave height 1.50 V, wave velocity 10 m/s; (d) wave height 1.50 V, wave velocity 3000 m/s

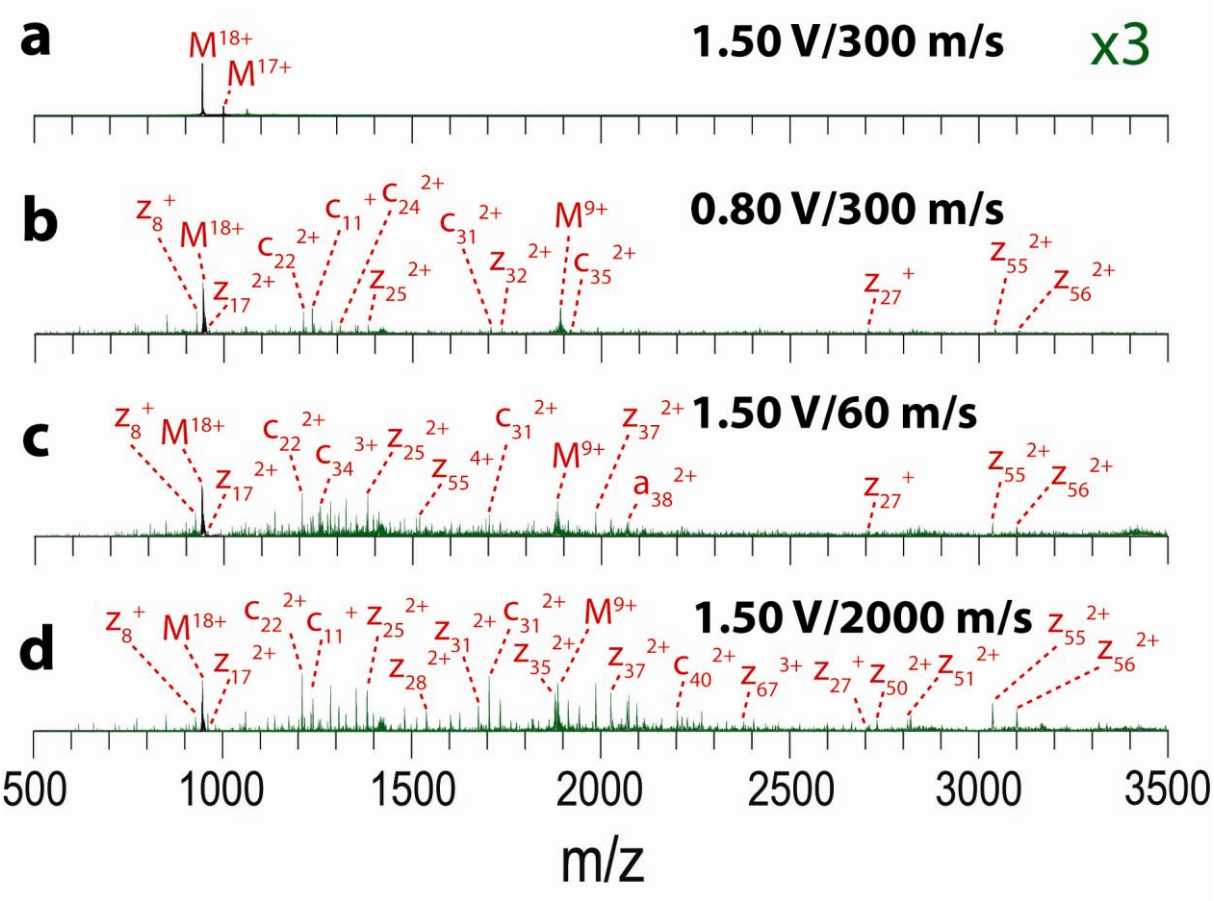

Top-down ETD spectra of myoglobin (18+) with (a) wave height 1.50 V, wave velocity 300 m/s; (b) wave height 0.80 V, wave velocity 300 m/s; (c) wave height 1.50 V, wave velocity 60 m/s; (d) wave height 1.50 V, wave velocity 2000 m/s

S-5 Drift time of Cs^+ (IM) versus log (WV)

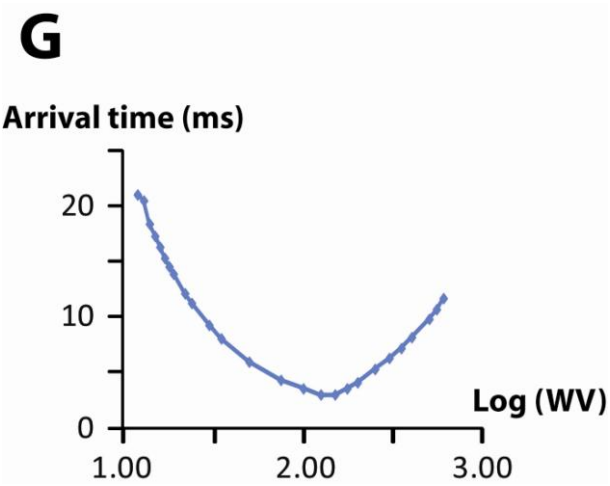

The wave height in the ion mobility cell was kept constant at 10 V, while the wave velocity was varied between 10 and 600 m/s. As expected, the arrival time reaches a minimum at an intermediate wave velocity (150 m/s; log (WV) = 2.2), and increases moving to either lower or higher velocity.

S-6 ETD products of substance P (3+): charge reduction vs. fragmentation with varying T-wave height and velocity

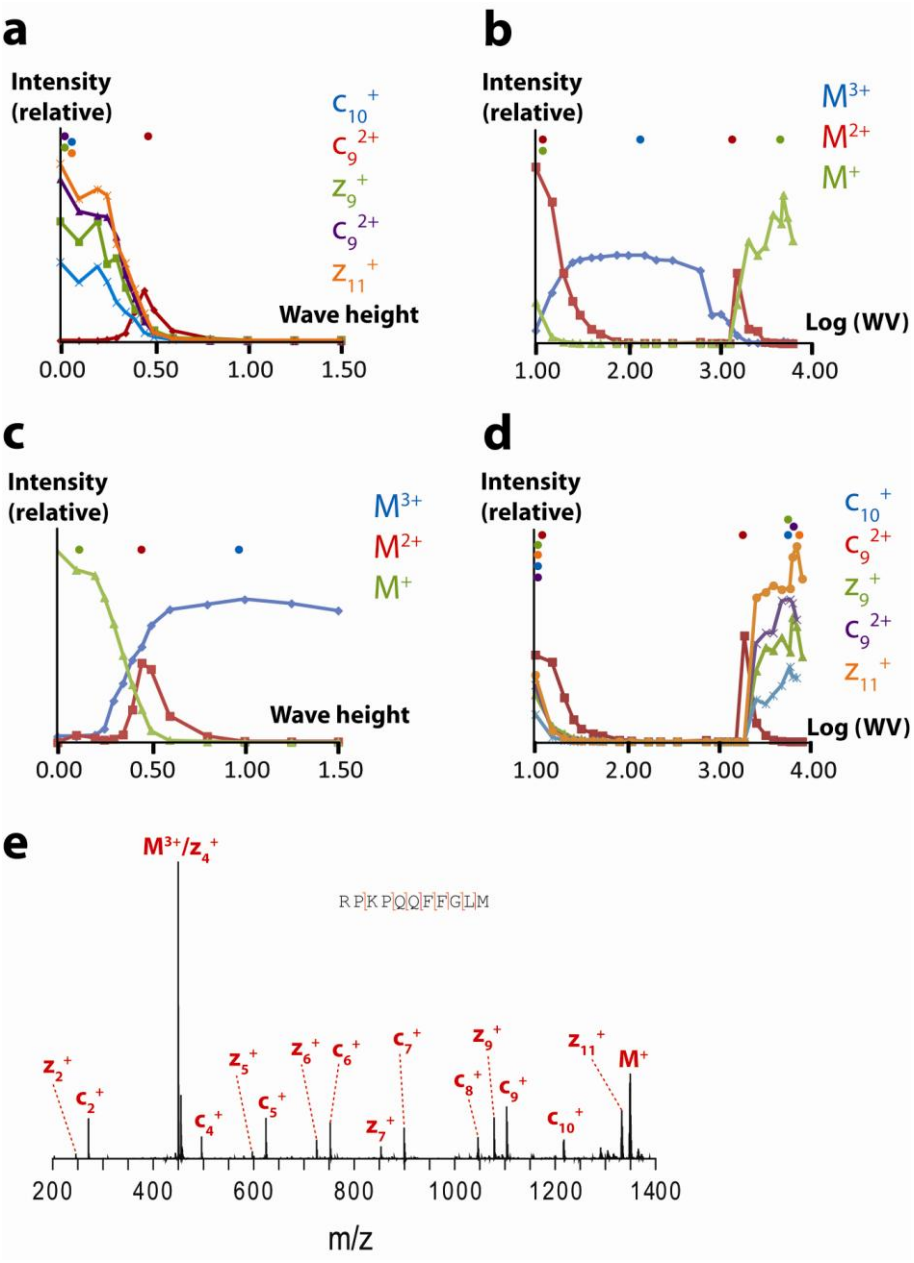

Plots of (a) nominal substance P charge states versus wave height (wave velocity = 300 m/s); and (b) log. wave velocity (wave height = 1.50 V); (c) selected substance P fragments versus wave height (wave velocity = 300 m/s); and (d) log. wave velocity (wave height = 1.50 V). Panel (e) shows a representative ETD spectrum for substance P, acquired at a wave height of 0.30 V and wave velocity of 300 m/s. The 3+ charge state was selected in the quadrupole in all cases.

S-7 Effect of the trap RF amplitude on (a) relative abundance of (reduced) charge states of the intact precursor and (b) fragmentation of 9+ ubiquitin

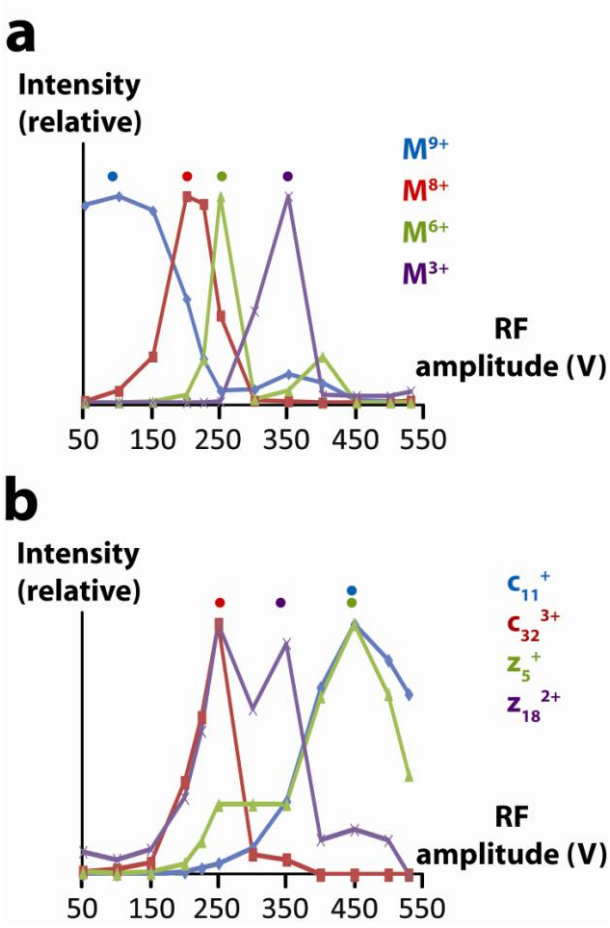

The trap T-wave height and velocity were kept constant at 0.50 V and 300 m/s, respectively, during these experiments. The normal operating regime for the trap RF amplitude in top-down ETD of proteins is 450 – 530 V.

S-8 Adduct formation between ubiquitin cations and 1,4-dicyanobenzene anions

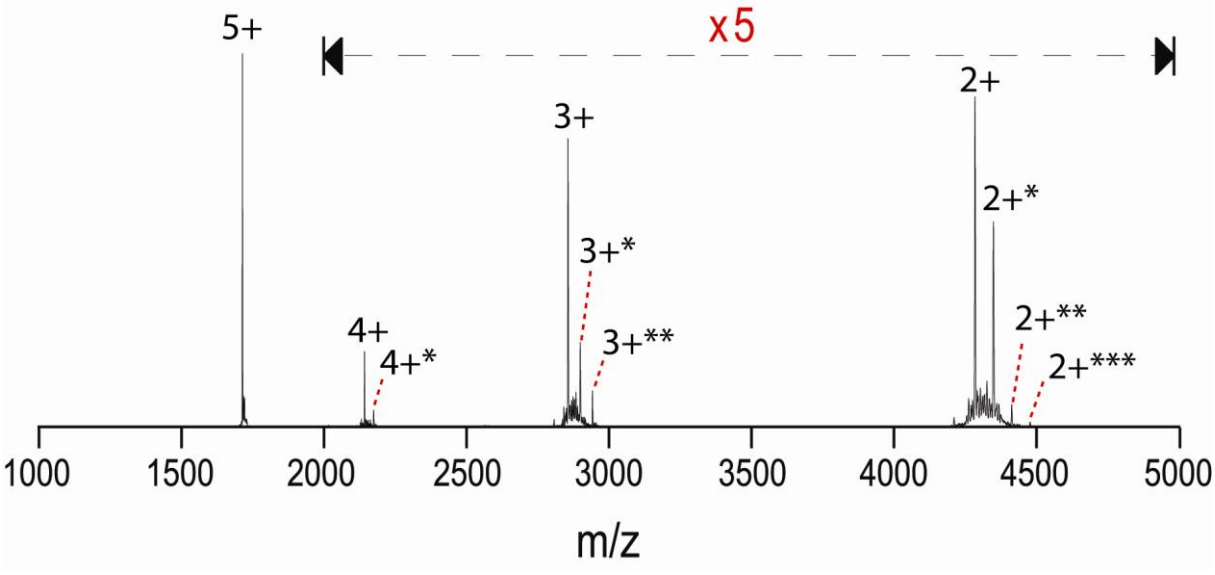

Formation of adducts with the ETD reagent can be observed during charge reduction of 5+ ubiquitin. The number of reagent anions in the complexes is indicated by asterisks.

S-9 Effect of variation of the reagent/analyte ion ratio

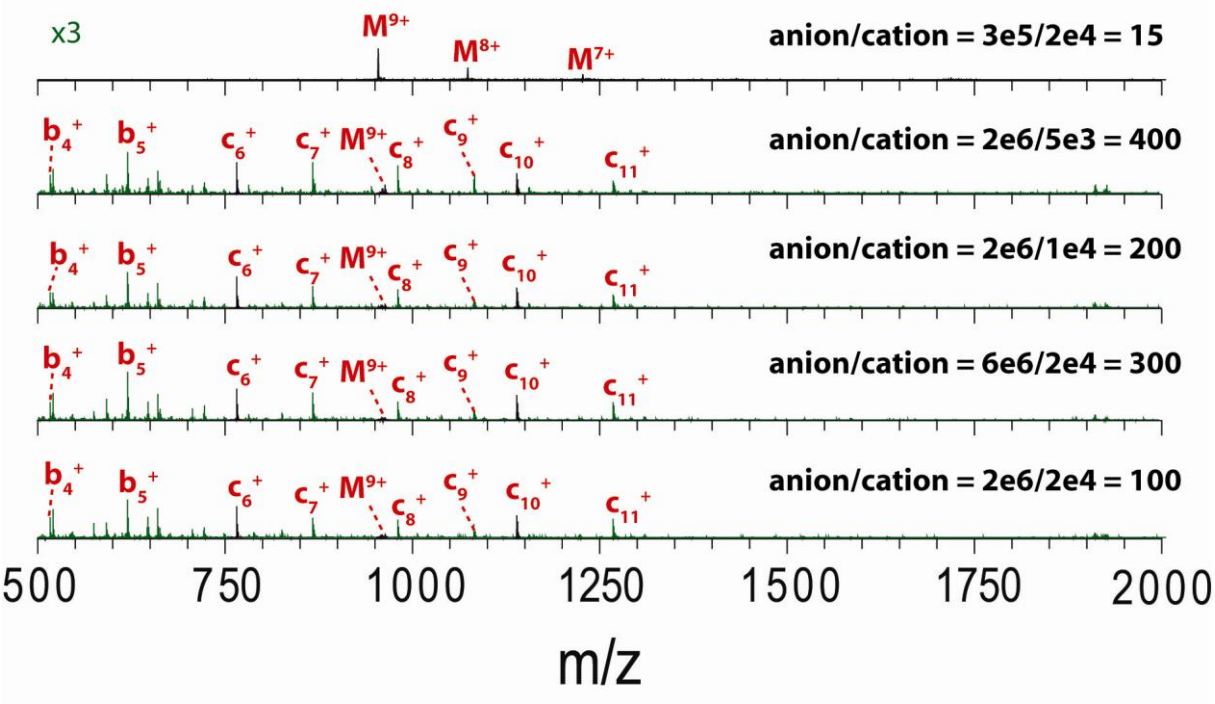

The four bottom spectra have a significant (>= 100-fold) reagent excess and all lead to similar spectra, showing efficient ETD fragmentation, even though both reagent and analyte counts, as well as their ratio are varied significantly. The top spectrum, with a reduced reagent/analyte ratio, only shows charge reduction, similar to how other tuning parameters reduce the 'effective' reagent concentration or reaction time